

See discussions, stats, and author profiles for this publication at: <https://www.researchgate.net/publication/40445019>

Hydrocarbon Metallosurfactants for CO₂

ARTICLE *in* LANGMUIR · DECEMBER 2009

Impact Factor: 4.46 · DOI: 10.1021/la903690c · Source: PubMed

CITATIONS

8

READS

38

9 AUTHORS, INCLUDING:



Julian Eastoe

University of Bristol

302 PUBLICATIONS 7,735 CITATIONS

[SEE PROFILE](#)



Robert M. Enick

University of Pittsburgh

199 PUBLICATIONS 3,486 CITATIONS

[SEE PROFILE](#)



Azmi Mohamed

Universiti Pendidikan Sultan Idris (UPSI)

39 PUBLICATIONS 266 CITATIONS

[SEE PROFILE](#)



Martin J Hollamby

Keele University

30 PUBLICATIONS 687 CITATIONS

[SEE PROFILE](#)

Hydrocarbon Metallosurfactants for CO₂

Kieran Trickett,[†] Dazun Xing,[‡] Julian Eastoe,^{*,†} Robert Enick[‡] Azmi Mohamed,[†] Martin J. Hollamby,[†] Stephen Cummings,[†] Sarah E. Rogers,[§] and Richard K. Heenan[§]

[†]School of Chemistry, University of Bristol, Cantock's Close, Bristol, BS8 1TS United Kingdom, [‡]National Energy Technology Laboratory IAES, and Department of Chemical and Petroleum Engineering, Swanson School of Engineering, University of Pittsburgh, 3700 O'Hara Street, Pittsburgh, Pennsylvania 15261, and [§]ISIS STFC, Rutherford Appleton Laboratory, Chilton, United Kingdom OX11 0QZ

Received September 30, 2009. Revised Manuscript Received November 16, 2009

Cobalt and nickel salts of the highly branched trichain anionic surfactant sodium 1,4-bis(neopentyloxy)-3-(neopentyloxycarbonyl)-1,4-dioxobutane-2-sulfonate (TC14) are shown to be soluble in dense CO₂ at concentrations up to 6 wt % at 500 bar pressure. This is a remarkably high solubility for such hydrocarbon transition metal surfactants in CO₂. High-pressure small-angle neutron scattering (HP-SANS) has been used to study the surfactant aggregates in a normal organic solvent, cyclohexane, dense CO₂, and also mixtures of these two pure solvents. The results show that transition metal TC14 derivatives are viable compounds for incorporating reactive and functional metal ions into CO₂.

Introduction

Carbon dioxide is an attractive alternative to conventional petrochemical solvents. It has many beneficial properties, including being nontoxic, nonflammable, inexpensive, and most importantly environmentally responsible.¹ However, CO₂ is a very weak solvent due to its low dielectric constant and zero dipole moment; as a result, most common solutes are insoluble in CO₂ or at best exhibit only weak solubility. The solvent properties could be improved by incorporation of CO₂-philic surfactants, and if these form reverse micelles then polar nanodomains will be generated.² Fluorinated surfactants^{3–6} and polymers⁷ have been shown to be the most suitable for CO₂ but suffer from the disadvantages of being environmentally persistent and expensive.⁸ Hydrocarbon alternatives have been reported, some with quite high CO₂ solubilities;^{9–12} however, these surfactants must be designed and custom-made to incorporate certain known CO₂-philic functional groups. Such effective hydrocarbon CO₂-philes include specialized highly branched^{9,10,12} or oxygenated surfactants.¹¹ Recently, it has been shown that a highly branched trichain surfactant, sodium 1,4-bis-(neopentyloxy)-3-(neopentyloxycarbonyl)-1,4-dioxobutane-2-sulfonate (TC14), aggregates and stabilizes hydrated reversed micelles in pure CO₂.¹² Here, two new TC14 analogues, Co(TC14)₂ and Ni(TC14)₂ (Figure 1), have been prepared, and the aggregation

behavior in high-pressure liquid CO₂ is investigated, with a view to applications as fluid property modifiers for CO₂.

The commercial potential of carbon dioxide is being realized in a variety of industries, including separation processes in the food industry, coatings, cleaning, and enhanced oil recovery (EOR).¹ However, its use in EOR is limited by the solvent low viscosity, and so developing CO₂-soluble hydrocarbon viscosity modifiers remains a live research challenge. The most successful viscosity enhancements of CO₂ have been achieved with custom-made compounds including fluorinated polymers,^{13,14} tri(semi-fluorinated alkyl) tin fluorides, and fluorinated telechelic ionomers.¹⁵ The self-assembly of surfactants into rodlike micelles is another way to induce viscosity increases.¹⁶ In fact, very recent results have shown that the formation of rodlike micelles is also possible in CO₂ using nickel or cobalt salts of the fluorinated surfactant di-HCF₄, generating viscosity enhancements of 90% compared to pure CO₂.¹⁷ That paper¹⁷ was the first example of a surfactant-based viscosity modifier in CO₂. Previous publications on Co²⁺ and Ni²⁺ AOT surfactants in alkane solvents^{18–20} proposed that the hydrated cation size is important for fine-tuning repulsive interactions between surfactant headgroups, and driving changes in micellar curvature. As such, larger divalent cations (Ni²⁺, Co²⁺) cannot approach the SO₃[−] headgroups as closely as smaller ions (Na⁺), therefore being less efficient at screening repulsion between ionic headgroups. The net effect is to favor aggregates with lower interfacial curvature, such as cylindrical reversed micelles.^{18–20}

- (1) Beckman, E. J. *Ind. Eng. Chem. Res.* **2003**, *42*, 1598.
- (2) Eastoe, J.; Gold, S.; Steyler, D. C. *Langmuir* **2006**, *22*, 9832.
- (3) Liu, Z. T.; Erkey, C. *Langmuir* **2001**, *17*, 274.
- (4) Lee, C. T.; Johnston, K. P.; Dai, H. J.; Cochran, H. D.; Melnichenko, Y. B.; Wignall, G. D. *J. Phys. Chem. B* **2001**, *105*, 3540.
- (5) Eastoe, J.; Paul, A.; Downer, A.; Steyler, D. C.; Rumsey, E. *Langmuir* **2002**, *18*, 3014.
- (6) Eastoe, J.; Cazelles, B. M. H.; Steyler, D. C.; Holmes, J. D.; Pitt, A. R.; Wear, T. J.; Heenan, R. K. *Langmuir* **1997**, *13*, 6980.
- (7) Eastoe, J.; Gold, S. *Phys. Chem. Chem. Phys.* **2005**, *7*, 1352.
- (8) Renner, R. *Science* **2004**, *306*, 1887.
- (9) Eastoe, J.; Paul, A.; Nave, S.; Steyler, D. C.; Robinson, B. H.; Rumsey, E.; Thorpe, M.; Heenan, R. K. *J. Am. Chem. Soc.* **2001**, *123*, 988.
- (10) Gold, S.; Eastoe, J.; Grilli, R.; Steyler, D. C. *Colloid Polym. Sci.* **2006**, *284*, 1333.
- (11) Eastoe, J.; Gold, S.; Rogers, S.; Wyatt, P.; Steyler, D. C.; Gurgel, A.; Heenan, R. K.; Fan, X.; Beckman, E. J.; Enick, R. M. *Angew. Chem., Int. Ed.* **2006**, *45*, 3675.
- (12) Hollamby, M.; Trickett, K.; Mohamed, A.; Cummings, S.; Tabor, R.; Myakunkaya, O.; Gold, S.; Rogers, S.; Heenan, R. K.; Eastoe, J. *Angew. Chem., Int. Ed.* **2009**, *48*, 4993.

- (13) Huang, Z.; Shi, C.; Xu, J.; Kilic, S.; Enick, R. M.; Beckman, E. J. *Macromolecules* **2000**, *33*, 5437.
- (14) Xu, J.; Wlaschin, A.; Enick, R. *SPE J.* **2003**, *8*, 85.
- (15) Shi, C. M.; Huang, Z. H.; Beckman, E. J.; Enick, R. M.; Kim, S. Y.; Curran, D. P. *Ind. Eng. Chem. Res.* **2001**, *40*, 908.
- (16) Trickett, K.; Eastoe, J. *Adv. Colloid Interface Sci.* **2008**, *144*, 66.
- (17) Trickett, K.; Xing, D.; Enick, R.; Eastoe, J.; Hollamby, M.; Mutch, K.; Rogers, S.; Heenan, R. K.; Steyler, D. *Langmuir*, published online Sept 24, <http://dx.doi.org/10.1021/la902128g>.
- (18) Eastoe, J.; Fragneto, G.; Robinson, B. H.; Towey, T. F.; Heenan, R. K.; Leng, F. *J. Chem. Soc., Faraday Trans.* **1992**, *88*, 461.
- (19) Eastoe, J.; Towey, T. F.; Robinson, B. H.; Williams, J.; Heenan, R. K. *J. Phys. Chem.* **1993**, *97*, 1459.
- (20) Eastoe, J.; Steyler, D. C.; Robinson, B. H.; Heenan, R. K.; North, A. N.; Dore, J. C. *J. Chem. Soc., Faraday Trans.* **1994**, *90*, 2497.

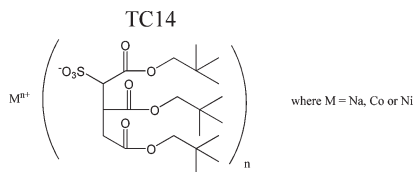


Figure 1. Structure of $M^{n+}(\text{TC14})_n$ where $M = \text{Na}^+, \text{Co}^{2+}$, and Ni^{2+} .

Given the environmental disadvantages⁸ associated with fluorinated compounds, there is an obvious need to find hydrocarbon alternatives which will also self-assemble to form viscosity-enhancing rodlike micelles in dense CO_2 . Here, the ability of $\text{Co}(\text{TC14})_2$ and $\text{Ni}(\text{TC14})_2$ (Figure 1) to aggregate in a typical organic solvent cyclohexane, pure CO_2 , and also in mixtures of the two solvents is assessed by small-angle neutron scattering (SANS). The results show that transition metal TC14 derivatives are viable compounds for solubilizing reactive and functional metal ions in CO_2 . These findings have the potential to open up new applications in fluid modification, lubrication, and reactivity of dense CO_2 .

Experimental Section

Surfactants. Synthesis, purification, and chemical characterization of the surfactant $\text{Na}(\text{TC14})$ have been previously described.¹⁰ $M^{2+}(\text{TC14})_2$ analogues were prepared from the sodium salt using a liquid–liquid ion exchange process, which has also been detailed elsewhere.^{18–20} Further information on characterization can be found in the Supporting Information.

Phase Behavior. For high-pressure experiments, a preweighed amount of surfactant was added to a pressure view cell. If required, an aliquot of water was added to give the desired water-to-surfactant ratio, $w = [\text{water}]/[\text{surfactant anion}]$. In all cases, the w value used in this work refers to the total level of water added to the system, but it has not been corrected for the small background solubility of water in CO_2 .²¹ In order to compare monovalent and divalent salts, the w value is defined with respect to surfactant anion concentration $[\text{TC14}^-]$. The pressure cell was then sealed and filled with liquid CO_2 at 100 bar via a syringe pump (Thar). Further adjustments to pressure were made using a piston, and samples were stirred for 10 min to attain equilibrium. Phase transitions were then determined visually by adjusting pressure at fixed temperature. In some cases, additional CO_2 was added to the system in order to assess the phase behavior over a range of surfactant concentrations. Reproducibility in the phase transitions (P_{Trans}) determined using different synthesized surfactant batches and by different operators using different pressure cells in different laboratories was typically ± 40 bar.

Small-Angle Neutron Scattering (SANS). The LOQ time-of-flight instrument, at the Rutherford Appleton Laboratory at ISIS UK, was used in conjunction with a stirred high-pressure cell (Thar; see the Supporting Information). For all experiments, the path length was 10 mm, the neutron beam diameter was 10 mm, pressure = 400 bar, and $T = 25^\circ\text{C}$. The measurements gave the absolute scattering cross section $I(Q)$ (cm^{-1}) as a function of momentum transfer Q (\AA^{-1}). The accessible Q range was $0.007\text{--}0.22\text{ \AA}^{-1}$, arising from an incident neutron wavelength of $2.2\text{--}10\text{ \AA}$. Absolute intensities ($\pm 5\%$) for $I(Q)$ (cm^{-1}) were determined by calibrating the received signal for a partially deuterated polymer standard. The data were normalized for transmission, empty cell, solvent background, and pressure induced changes in cell volume as before.²⁶

Neutrons are scattered by short-range interactions with sample nuclei, with the “scattering power” of different components being

defined by a scattering-length density (SLD), ρ (cm^{-2}). For liquid CO_2 , $\rho_{\text{CO}_2} \sim 2.50 \times \text{mass density} \times 10^{10} \text{ cm}^{-2}$.²² At the experimental pressure of 400 bar, the CO_2 density is $\sim 1.0 \text{ g cm}^{-3}$ so that $\rho_{\text{CO}_2} \sim 2.5 \times 10^{10} \text{ cm}^{-2}$. The contrast ($\rho_{\text{CO}_2} - \rho_{\text{TC14}/\text{H}_2\text{O}}$) was provided by using a hydrogen containing surfactant (H-surfactant) with H_2O and was calculated as a linear combination of contributions from the H-surfactant (assuming density 1.1 g cm^{-3} gives $\rho_{\text{TC14}} = 0.812 \times 10^{10} \text{ cm}^{-2}$) and where necessary H_2O ($\rho_{\text{H}_2\text{O}} = -0.56 \times 10^{10} \text{ cm}^{-2}$), taken to distribute within the surfactant micelles. For SANS experiments using mixtures of deuterated cyclohexane (C_6D_{12}) and CO_2 , the SLD of the mixed solvent ($\rho_{\text{CO}_2/\text{C}_6\text{D}_{12}}$) was calculated as a first order summation, weighted by the different volume fractions. The amount of water in the micelles was adjusted for the known solubility of water in CO_2 (at 400 bar $\sim 0.15\text{--}0.16 \text{ wt } \%$).²¹ Samples in pure CO_2 were run at a constant surfactant concentration of 2 wt %.

For SANS experiments carried out at ambient pressure, neutron contrast was provided with H-surfactant and H_2O (where applicable) against the solvent deuterated cyclohexane ($\rho_{\text{C}_6\text{D}_{12}} = 6.687 \times 10^{10} \text{ cm}^{-2}$). Surfactant concentration was 0.10 mol dm^{-3} , and samples were run at 25°C in 2 mm Hellma quartz cells and corrected for the cell and C_6D_{12} backgrounds as before.²³

Results

High-Pressure Studies in Pure CO_2 . $\text{Na}(\text{TC14})$ is considered to be an excellent surfactant for CO_2 ; it has three *t*-butyl tipped chains which have the effect of dramatically enhancing CO_2 compatibility.^{10,12} Importantly, $\text{Na}(\text{TC14})$ is soluble in CO_2 at less extreme conditions than the structurally related *t*-butyl tipped dichain surfactant AOT4⁹ (bis(3,5,5-trimethyl-1-hexyl) sulfosuccinate) and is more easily synthesized than other CO_2 -phillic oxygenated surfactants.¹¹ In pure CO_2 , changing the counterion from Na^+ to Co^{2+} and Ni^{2+} did not have a significant effect on surfactant solubility (phase behavior plots can be found in the Supporting Information, Figures S2 and S3). Both divalent salts of TC14 were remarkably CO_2 soluble, even though they are nonfluorous organometallic compounds, demonstrating that the branched trichain structure is a flexible CO_2 -phillic motif, capable of solubilizing different surfactant headgroup and counterion structures. All surfactants were able to stabilize small amounts of water ($w = 5$), which increased P_{Trans} by approximately 100 bar (Figure S3, Supporting Information) over the dry systems ($w = 0$). These higher pressures, and densities, reflect the additional CO_2 solvent strength required to solubilize micelles swollen with increasing amounts of water.²

Previously, only one other nonfluorous organometallic surfactant has been reported to have any significant CO_2 solubility:^{24–26} (Ag-AOT4), being the silver salt of the *t*-butyl tipped dichain AOT4. In those papers, Ag-AOT4 was used as a metal precursor, which was reduced in CO_2 in the presence of a capping agent isostearic acid, in order to generate silver nanoparticles in CO_2 media.^{24–26} Figure 2 shows solubility curves for both $\text{Co}(\text{TC14})_2$ and $\text{Ni}(\text{TC14})_2$ in pure CO_2 , along with literature data for Ag-AOT4²⁶ and a fluorinated analogue, $\text{Ni}(\text{di-HCF4})_2$.¹⁷ Even though they are hydrocarbon surfactants, at 500 bar, the organometallic trichain TC14 derivatives all exhibit remarkable CO_2

(22) McClain, J. B.; Londono, D.; Combes, J. R.; Romack, T. J.; Canelas, D. A.; Betts, D. E.; Wignall, G. D.; Samulski, E. T.; DeSimone, J. M. *J. Am. Chem. Soc.* **1996**, *118*, 917.

(23) Nave, S.; Eastoe, J.; Heenan, R. K.; Steytler, D.; Grillo, I. *Langmuir* **2000**, *16*, 8741.

(24) Bell, P. W.; Amand, M.; Fan, X.; Enick, R. M.; Roberts, C. B. *Langmuir* **2005**, *21*, 11608.

(25) Anand, M.; Bell, P. W.; Fan, X.; Enick, R. M.; Roberts, C. B. *J. Phys. Chem. B* **2006**, *110*, 14693.

(26) Fan, X.; McLeod, M. C.; Enick, R. M.; Roberts, C. B. *Ind. Eng. Chem. Res.* **2006**, *45*, 3343.

(21) Harrison, K.; Goveas, J.; Johnston, K. P.; O'Rear, E. A. *Langmuir* **1994**, *10*, 3536.

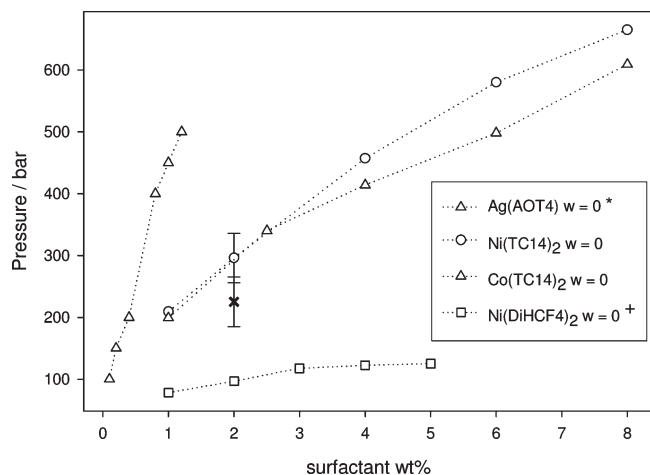


Figure 2. Phase diagram in pure CO₂ showing effect of surfactant concentration on P_{Trans} . $w = 0$ and $T = 25^\circ\text{C}$. (*) Data from ref 26 and (+) data from ref 17. Point marked \times (Ni(TC14)₂, $w = 0$) represents a repeat conducted, with a different surfactant batch, in a different pressure cell and by a different operator, representing uncertainties of ± 40 bar as shown by the error bars.

solubilities (6 wt % up to 500 bar). This is 6 times the level for Ag-AOT4 under similar conditions²⁶ but notably far less than the fluorinated nickel analogue Ni(di-HCF4)₂.¹⁷

Although not the focus of this paper, metallosurfactants of the type described here have the potential to be used in the synthesis of nanoparticles. Clearly, this recently developed CO₂-soluble trichain surfactant template TC14 appears to have some advantages over the Ag-AOT4 previously reported, given lower transition pressures (P_{Trans}), greater maximum solubility, and the ability to stabilize small amounts of water. Although these TC14 surfactants are not as good CO₂-philes as the related fluorinated Ni(di-HCF4)₂, they are certainly more economical and environmentally friendly.¹²

Due to the range of neutron wavelengths available, SANS is suitable for studying the shapes and sizes of colloidal systems.²⁷ High-pressure small-angle neutron scattering (HP-SANS) is a particularly important technique for determining surfactant aggregation structures in liquid CO₂.² The SANS profile can be useful in determining the presence of anisotropic particles. In the low Q region (typically $< 0.10 \text{ \AA}^{-1}$), the scattering may scale as $I(Q) \sim Q^{-D}$, where D is a characteristic “fractal dimension” for the dispersed aggregates; hence, the gradient of a log–log plot will be $-D$. For noninteracting spheres, a log–log plot has a zero slope in this low Q region, whereas rods will follow a power-law decay of -1 , characteristic of a one-dimensional assembly.²⁷

Owing to high pressure cell safety limits, all experiments were conducted at 400 bar in clear one phase regions, and in terms of P_{Trans} far from any phase boundaries. It should be noted that these are challenging HP-SANS experiments, being of low concentration, small aggregate radius (10–20 Å), and low neutron contrast ($\Delta\rho \approx 2 \times 10^{10} \text{ cm}^{-2}$ in CO₂) making the intensities, $I(Q)$, much lower than those seen in the deuterated C₆D₁₂ systems studied.

Figure 3 shows SANS profiles for dry and hydrated micelles of Ni(TC14)₂ and Co(TC14)₂ in CO₂. The $I(Q)$ curves are characteristic of reverse micelles in low dielectric solvent media, and the $I(Q)$ increases on addition of water are consistent with increasing volume fractions, as expected for progressively hydrated micelles. This general behavior is identical to that seen

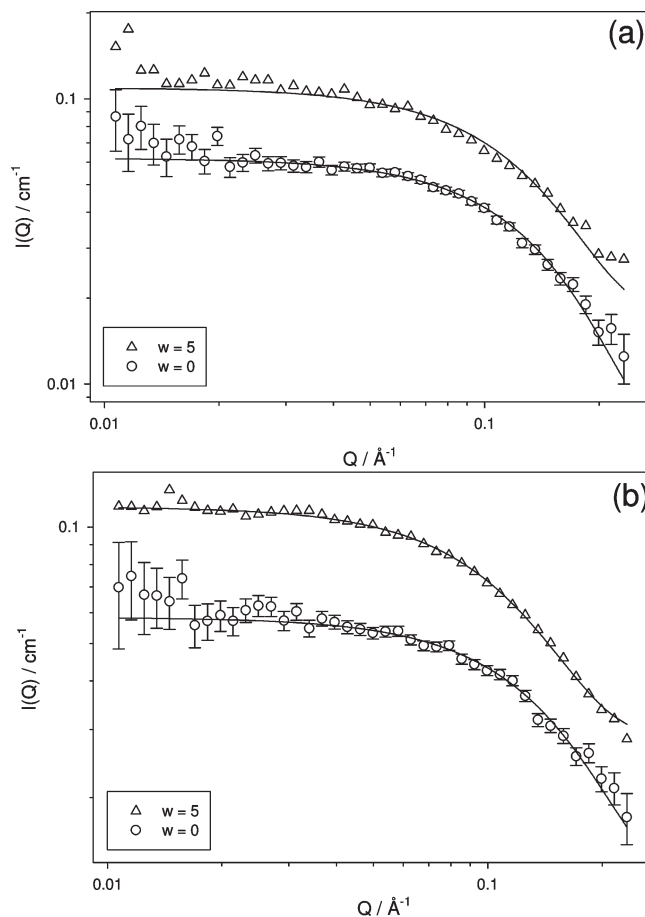


Figure 3. SANS profiles for $w = 0$ and $w = 5$: (a) Co(TC14)₂ and (b) Ni(TC14)₂ in pure CO₂. [Surfactant] = 0.04 mol dm^{-3} ($\sim 2 \text{ wt } \%$), pressure = 400 bar, and $T = 25^\circ\text{C}$. Lines through data points are model fits, and parameters are listed in Table 1. Characteristic error bars are shown for the lowest intensity samples.

Table 1. Fitted Parameters from SANS Data in Pure CO₂

surfactant	w	radius/Å ± 2 Å
Na TC14	0	11
	5	12
Co(TC14) ₂	0	11
	5	13
Ni(TC14) ₂	0	11
	5	13

previously for Na(TC14).¹² The absence of any logarithmic decay in the low Q region indicates that the micelles must be essentially spherical, and surprisingly given the previous studies using analogous divalent ion sulfosuccinate surfactants in cyclohexane^{17–20} there is no evidence for anisotropic structures in terms of exponential scattering. In all cases, the data were quantitatively fitted using a Schultz distribution of polydisperse spheres. Good fits, with physically realistic parameters, were obtained for the three surfactants, and fitted parameters are detailed in Table 1. The safe operating limit of the pressure cell was 400 bar, and below this pressure it was not possible to investigate systems with $w > 5$.

Ambient Pressure Studies in C₆D₁₂. Parallel SANS experiments in C₆D₁₂ were conducted and compared to those in dense CO₂. For both the dry and hydrated micelles of the Na⁺ salt of TC14 in cyclohexane, the absence of any logarithmic decay in the data is consistent with the presence of small spherical particles.

(27) Eastoe, J. *Surfactant Chemistry*; Wuhan University Press: Wuhan, 2003.

Table 2. Fitted Parameters to SANS Data in Pure C₆D₁₂^a

surfactant	w	radius/Å ± 2 Å	length/Å (rods only) ± 5 Å
Na(TC14)	0	11	
	5	16	
Co(TC14) ₂	0	11	
	5	14	100
	10	18	320
	15	22	270
Ni(TC14) ₂	0	12	
	5	14	130
	10	19	350
	15	24	225

^a w values 0–15 were studied except in the case of Na(TC14) where w = 5 was the maximum value stable at room temperature.

The data were quantitatively fitted using a Schultz distribution of spherical particles (scattering laws are given in the Supporting Information). The fitted parameters are detailed in Table 2, and the scattering profiles can be found in the Supporting Information (Figure S4): higher w values were not studied, being unstable at room temperature. The scattering profiles for the Na⁺ salt of TC14 in C₆D₁₂ were broadly the same as those seen in CO₂¹² and consistent with essentially spherical aggregates of similar radii.

Figure 4 shows the scattering profiles for Ni(TC14)₂ and Co(TC14)₂ in C₆D₁₂ over a range of w values. For the dry micelles, there is no evidence for logarithmic scattering, and as with the dry micelles of Na(TC14) the SANS data are well represented by a spherical form factor with radius 11 ± 2 Å. However, on increasing w, the scattering profiles for the Co²⁺ and Ni²⁺ salts are very different from that of the Na⁺ analogue, with the low Q region (Q < 0.10 Å⁻¹) showing a greater logarithmic component with increasing w. For w = 10, the intensity, I(Q), scales as approximately Q⁻¹, which is characteristic of rodlike micelles. The data for the hydrated micelles and microemulsion systems (w = 5, 10, 15) were found to be well represented by a rod form factor. The fitted parameters for rod radius and length are listed Table 2. The results are consistent with addition of water to micelles of Co(TC14)₂ and Ni(TC14)₂, inducing a sphere-to-rod transition. This is distinctly different from the behavior of Na(TC14), for which the micelles are always spherical and simply swell in size with added water (at least up to the maximum value studied).

Based on standard packing parameter arguments,²⁷ it might have been expected that a highly branched trichain surfactant, with extensive hydrocarbon bulk, would have a greater tendency to bend about water, hence favoring high curvature structures. However, the behavior of the divalent salts of TC14 in C₆D₁₂ is remarkably similar to that of the analogous double chain AOT surfactant in the same solvent^{18–20} and the fluorinated surfactant di-HCF₄ in dense-CO₂.¹⁷ Note that this behavior contrasts with that for the divalent salts of TC14 in dense CO₂, where the exchange of counterion did not induce a sphere-to-rod transition; conceivably, this may be due to the small amounts of dispersed water. In the ambient pressure C₆D₁₂ system, the rodlike aggregates were most evident at w = 10.

High-Pressure: Mixed Solvents CO₂/C₆D₁₂. To assess the aggregate structures at higher w values, where rodlike micelles are more likely to form, it was necessary to improve the solvent quality of CO₂ by adding small amounts of an alkane cosolvent. Both C₆D₁₂ and CO₂ are miscible at the compositions employed, and it is assumed that a homogeneous mixed solvent forms. The

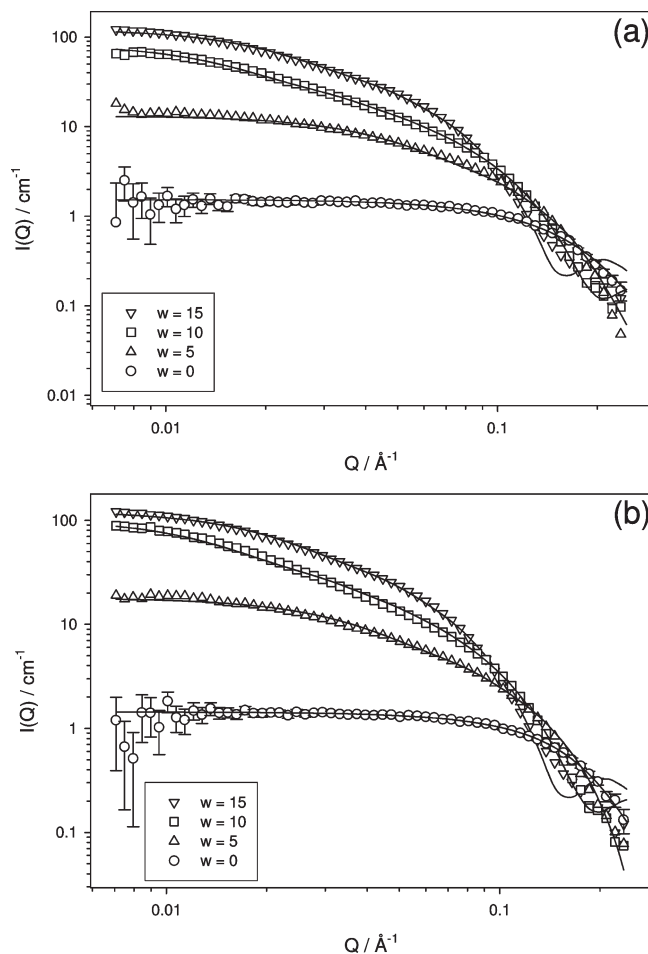


Figure 4. SANS profiles for (a) Co(TC14)₂ and (b) Ni(TC14)₂ in pure C₆D₁₂ showing changes in aggregate structure with increasing w value. [Surfactant] = 0.10 mol dm⁻³. Lines through data points are model fits, and parameters are listed in Table 2. Characteristic error bars are shown for the lowest intensity samples.

use of cosolvents to improve the solvent power is well-known in enhancing solubility in CO₂,²⁸ having also been recently applied to micellar systems.²⁹ Prior to injection of CO₂, C₆D₁₂ (12 wt %) was added to the pressure cell along with the required amount of surfactant and water. For all systems studied, the addition of 12 wt % C₆D₁₂ had the effect of reducing P_{Trans} by between 100 and 200 bar depending on the system (see the Supporting Information, Figure S3). The upshot of adding this fraction of C₆D₁₂ was that samples formulated at w = 10 were now stable, as compared to the unstable systems in pure CO₂ under these operating conditions. w values greater than 10 were not stable in the solvent mixture under these T and P conditions.

Again, HP-SANS was used to investigate the aggregate structures in these liquid CO₂/C₆D₁₂ mixtures. SANS profiles for Ni(TC14)₂, Co(TC14)₂, and Na(TC14) at various w values are shown in Figure 5. Surprisingly, the scattering was still characteristic of spherical aggregates, being reminiscent of the results found in pure CO₂ (Figure 3) but very different from those found in pure C₆D₁₂ (Figure 4). All data sets could be fitted to the Schultz polydisperse spheres model (fit parameters in Table 3), and the radii of the spherical droplets were comparable to those obtained for Na(TC14) in pure C₆D₁₂. It was evident that for these trichain surfactants in CO₂/C₆D₁₂ mixtures that the exchange of

(28) Walsh, J. M.; Ikononou, G. D.; Donohue, M. D. *Fluid Phase Equilib.* **1987**, *33*, 295.

(29) Hollamby, M.; Trickett, K.; Mohamed, A.; Eastoe, J.; Rogers, S.; Heenan, R. K. *Langmuir* **2009**, *25*, 12909–12913.

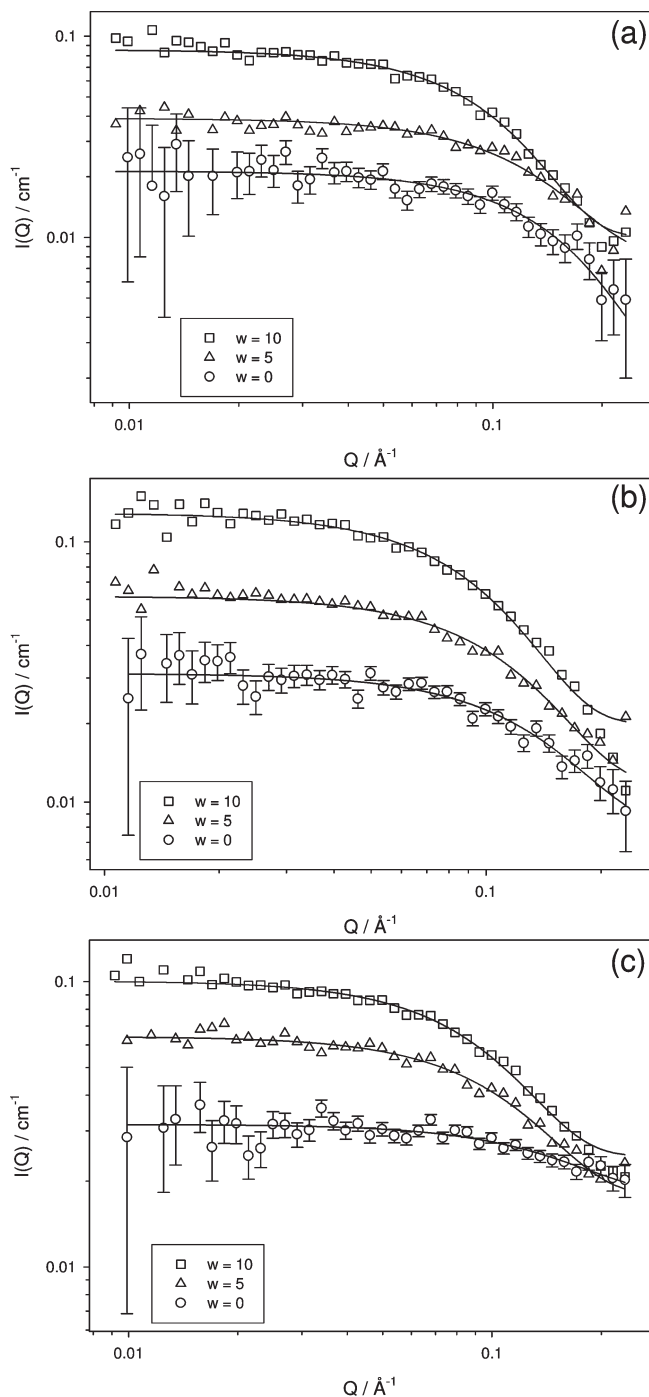


Figure 5. SANS profiles for $w = 0, 5$ and 10 in $\text{CO}_2/\text{C}_6\text{D}_{12}$ (12 wt %) mixtures for (a) $\text{Na}(\text{TC14})$, (b) $\text{Ni}(\text{TC14})_2$, and (c) $\text{Co}(\text{TC14})_2$. [Surfactant] = 0.04 mol dm^{-3} ($\sim 2 \text{ wt } \%$), pressure = 400 bar, and $T = 25^\circ \text{C}$. Lines through data points are model fits, and parameters are listed in Table 3. Data in all cases show small spherical aggregates. Characteristic error bars are shown for the lowest intensity sample.

counterion is not able to affect the aggregate structure, in opposition to the observations made in pure C_6D_{12} (Figure 4).

To investigate this further, HP-SANS experiments were conducted whereby a C_6D_{12} -continuous $\text{Ni}(\text{TC14})_2$ stabilized microemulsion, known to form rodlike micelles, was placed in the pressure cell. The microemulsion completely covered the cell windows, but the cell was only partly filled, leaving a vacant head space. The scattering profile was recorded and, as expected, was

Table 3. Fitted Parameters for SANS Data in $\text{CO}_2/\text{C}_6\text{D}_{12}$ (12 wt %) Mixtures

surfactant	w	radius/ $\text{\AA} \pm 2 \text{\AA}$
$\text{Na}(\text{TC14})$	0	11
	5	13
	10	17
$\text{Co}(\text{TC14})_2$	0	11
	5	14
	10	17
$\text{Ni}(\text{TC14})_2$	0	12
	5	14
	10	17

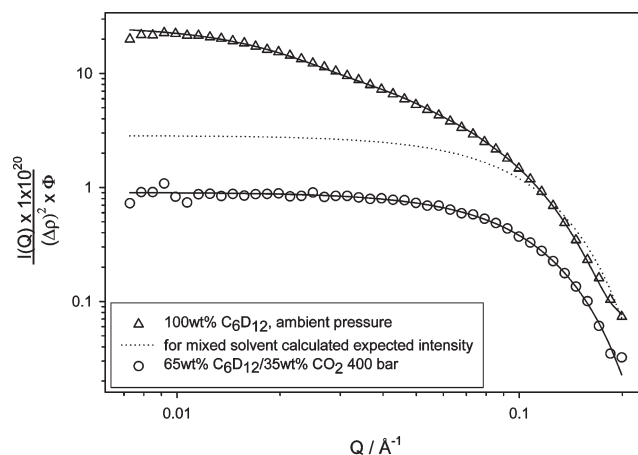


Figure 6. SANS profiles for $\text{Ni}(\text{TC14})_2$ $w = 10$ comparing two different solvents: 100 wt % C_6D_{12} and a solvent mixture 65 wt % $\text{C}_6\text{D}_{12}/35 \text{ wt } \%$ CO_2 . $T = 25^\circ \text{C}$. Lines through data points are model fits, and parameters are listed in Table 4. SANS intensity has been corrected for the change in volume fraction (Φ) and the difference in scattering length density ($\Delta\rho^2$) that occurred on introducing liquid CO_2 to the system.

Table 4. Fitted Parameters to SANS Data in Solvent Mixtures of Different Compositions

surfactant	solvent	radius/ $\text{\AA} \pm 2 \text{\AA}$	length/ \AA (rods only) $\pm 5 \text{\AA}$
$\text{Ni}(\text{TC14})_2$	100 wt % C_6D_{12}	18	240
$\text{Ni}(\text{TC14})_2$	65 wt % $\text{C}_6\text{D}_{12}/35 \text{ wt } \%$ CO_2	16	

shown to be characteristic of rodlike micelles (Figure 6, Table 4 details the fitted parameters). Dense CO_2 was then pumped in to fill the vacant head space, and the mixture was vigorously stirred, resulting in a homogeneous mixed solvent (approximately 65 wt % C_6D_{12} and 35 wt % CO_2). The introduction of liquid CO_2 into this originally C_6D_{12} solvent microemulsion had two distinct effects on the SANS profiles: first, there was a rod-to-sphere transition, and second a reduction in scattering intensity was noted.

Obviously, introduction of liquid carbon dioxide resulted in a decrease in surfactant concentration and a very small reduction in the quantity of dispersed water (given that water has a limited solubility in CO_2).²¹ However, both of these effects are together too small to explain the change in aggregate structure. Furthermore, nor do they explain the reduction in SANS intensity, as the data have been corrected for the changes in volume fraction (Φ) and differences in scattering length density ($\Delta\rho^2$) incurred on introducing liquid CO_2 . Given these corrections, the observed

SANS intensity for the mixed solvent system is still 3 times lower than that expected for a spherical micelle of this composition. This lower than expected scattering intensity was observed for all similar studies involving TC14 in CO₂ or CO₂/C₆D₁₂ mixed solvents. The change in structure from spheres to rods was also evident with another hydrocarbon surfactant (Ni(AOT4)₂). With this surfactant, it was also shown that pressurizing the pure C₆D₁₂ system had no effect on the aggregate structure (Figure S5 and Table S1 in the Supporting Information).

Above, it was shown that in a typical liquid hydrocarbon C₆D₁₂ the trichain surfactant TC14 will self-assemble to form rodlike aggregates upon exchange of surfactant counterion from sodium to either cobalt or nickel. This observation has been previously reported with divalent salt surfactants such as the commercially available surfactant AOT^{18–20} in hydrocarbon oils, and importantly now also in fluorocarbon surfactants in pure CO₂.¹⁷ The fact that trichain surfactants do not behave similarly in CO₂/C₆D₁₂ mixtures can therefore not exclusively be a consequence of the change in solvent to CO₂, but perhaps points to differences in the behavior of hydrocarbon and fluorocarbon surfactants in these systems.

It is interesting to speculate on the possible reasons for the observed micellar shape change. Simulations have shown that the fluorocarbon tails occupy a greater volume and cross-sectional area than equivalent hydrocarbon surfactants.^{30,31} As a consequence, the penetration of CO₂, itself with a small molecular volume, into the tail region is believed to be greater for hydrocarbon surfactants.^{30,31} A plausible explanation for the difference in aggregate structure (cylinders in C₆D₁₂ but spheres in CO₂) is if there were a greater penetration of CO₂, compared to C₆D₁₂, into the chain regions. This solvent partitioning would favor formation of spherical aggregates, driving the curvature more negative by preferentially swelling surfactant tails with CO₂. The effect of solvent penetration into dichain surfactant layers at model reverse curvature water-in-oil microemulsion interfaces has been previously been explored.³² The results indicated that the more compact cyclohexane molecule ($V_{\text{m}}^{\text{cyclo}} \sim 180 \text{ \AA}^3$) penetrated further into surfactant tails compared to the more bulky heptane molecules ($V_{\text{m}}^{\text{hept}} \sim 240 \text{ \AA}^3$, $\Delta V_{\text{m}} \sim 60 \text{ \AA}^3$).³² Although the observed difference in penetration was small in that case, here the expected effect would be even more significant given the greater difference in molecular volume between cyclohexane and CO₂ ($V_{\text{m}}^{\text{CO}_2} = 70 \text{ \AA}^3$, $\Delta V_{\text{m}} = 110 \text{ \AA}^3$).

The reduction in SANS intensity could be due to the difference in scattering length density being smaller than expected. Given that the difference in the magnitude of expected and observed intensity is a factor of 3, this seems unlikely. Alternatively, the difference in intensity may suggest a partitioning of the surfactant away from the CO₂/water interface and micelles into the bulk. In other words, there would be a solvent-induced increase in the effective “cmc”, enhancing solubility of the free molecules and leaving a smaller proportion available to form aggregates. Previously, high-pressure surface tension measurements using fluorinated surfactants have shown a lower packing density at the water/CO₂ interface when compared to air/water and water/oil interfaces.^{6,33–35} Given the

difficulties in collecting accurate high-pressure surface tension data, few studies have compared the behavior of analogous fluorocarbon and hydrocarbon surfactants at the water/CO₂ interface.³³ Furthermore, it is not clear from these experiments whether the penetration of small CO₂ molecules or increased monomer levels, or a combination of the two, is responsible for the change in aggregate structure from rods to spheres.

Conclusions

Recently, Co²⁺ and Ni²⁺ salts of the fluorinated dichain sulfosuccinate surfactant di-HCF4 have been shown to act as viscosity modifiers in CO₂ through formation of rodlike micelles.¹⁷ Another recent publication has detailed how the trichain hydrocarbon surfactant Na(TC14) is soluble and aggregates in pure CO₂.¹² This current work combines these ideas and assesses the ability of two new surfactant analogues, Co(TC14)₂ and Ni(TC14)₂, to form rodlike micelles in CO₂. A hydrocarbon surfactant which forms rodlike micelles has the potential to act as a viscosity modifier overcoming the environmental disadvantages associated with fluorinated additives,⁸ and therefore having potentially important ramifications for enhanced oil recovery.

In organic solvents, the custom-made divalent salts of the trichain surfactant TC14 behave much like the direct analogues of commercially available AOT. The growth of rodlike micelles can be induced by addition of water to dry micelles, stabilized by Co²⁺ and Ni²⁺ salts of TC14. Evidence has been provided for the formation of dry and hydrated micelles in both pure CO₂ and CO₂/C₆D₁₂ mixtures. However, SANS results suggest these surfactants in mixed CO₂/C₆D₁₂ solvents form spherical aggregates, and not rodlike aggregates which were observed in pure C₆D₁₂. As analogous fluorinated surfactants have been shown to form rodlike micelles in CO₂, this is not an effect purely due to the solvent. Hence, the challenge of developing a hydrocarbon-only viscosity modifier for CO₂ still remains.

However, importantly, two new hydrocarbon metallosurfactants have been shown to be soluble in pure CO₂ at high concentrations. This is a significant development given the low CO₂ compatibility of the majority of commercially available hydrocarbon surfactants. The surfactants described here offer advantages over the only other transition metal surfactant to be reported to be soluble in CO₂.^{24–26} These include having mild solubility conditions at lower pressures, a greater maximum solubility, and being able to disperse small amounts of water. The ability to incorporate metallosurfactants in CO₂ has potential implications in nanoparticle synthesis in CO₂, lubricants for dense CO₂, catalysis, and modification of CO₂ fluid properties through the incorporation of ionic species and polar moieties.

Acknowledgment. This technical effort was performed in support of the National Energy Technology Laboratory’s ongoing research in oil and gas under RDS Contract M2264 subtask 606.08.09.214. K.T., A.M., and M.J.H. thank the EPSRC, the Malaysian Government, Kodak and School of Chemistry at the University of Bristol for the provision of Ph.D. scholarships. S.C. thanks the EPSRC for a Ph.D. scholarship under the Next Generation Facility User scheme (EP/F020686). The ISIS-STFC Neutron Scattering Facility (formerly CCLRC) is thanked for the provision of beamtime. The EPSRC is thanked for provision of funding under Grants EP/C523105/1 and EP/F020686.

Supporting Information Available: Additional details of surfactant synthesis, purity, phase behavior, calculations, and SANS model fitting. This material is available free of charge via the Internet at <http://pubs.acs.org>.

(30) Stone, M. T.; Smith, P. G.; da Rocha, S. R. P.; Rossky, P. J.; Johnston, K. P. *J. Phys. Chem. B* **2004**, *108*, 1962.

(31) Stone, M. T.; da Rocha, S. R. P.; Rossky, P. J.; Johnston, K. P. *J. Phys. Chem. B* **2003**, *107*, 10185.

(32) Bumajdad, A.; Eastoe, J.; Heenan, R. K.; Lu, J. R.; Steytler, D. C.; Egelhaaf, S. J. *Chem. Soc., Faraday Trans.* **1998**, *94*, 2143.

(33) Dickson, J. L.; Smith, P. G.; Dhanuka, V. V.; Srinivasan, V.; Stone, M. T.; Rossky, P. J.; Behles, J. A.; Keiper, J. S.; Xu, B.; Johnson, C.; DeSimone, J. M.; Johnston, K. P. *Ind. Eng. Chem. Res.* **2005**, *44*, 1370.

(34) Da Rocha, S. R. P.; Johnston, K. P. *Langmuir* **2000**, *16*, 3690.

(35) Eastoe, J.; Bayazit, Z.; Martel, S.; Steytler, D. C.; Heenan, R. K. *Langmuir* **1996**, *12*, 1423.